# Where must we place obstacles in a flow to minimize its rate ?

François Bouchon & Laurent Chupin
Université Clermont Auvergne, CNRS, LMBP, F-63000 Clermont-Ferrand, France

5 septembre 2024

**Abstract** – We propose a numerical method in order to determining how to place fixed obstacles in a Stokes flow, for which the inlet constraint force is imposed, so that the flow rate is minimised. To do this, we study the shape derivative associated to such a Stokes flow, and we propose a descent algorithm. We first consider the case of spherical obstacles, and then general rigid obstacles for which the orientation must be taken into account. Numerical simulations complete the study.

## 1 Introduction

We consider an optimisation problem consisting in finding the position of rigid obstacles in a flow so that the flow rate is optimal (here we minimise the flow rate), considering that the inlet constraint force is imposed.
Some of the possible applications of this work can be the detection of risks of blockage in a conduit, or the design of structures in a river with a view to minimising the risks of natural damage.
As a first approach, we consider in this work that the flow is described by the Stokes system of equations, with adherence boundary condition on the obstacles as well as on the lateral parts of the flow. Moreover, we impose the inlet constraint force on one of the entries of the domain and we assume that this inlet constraint vanishes on the other part.
Although the obstacles are supposed to be rigid, we use some classical shape optimisation tools (see [7], [8], [13], [18], [20]) to derive an iterative numerical method to find the optimal position.
Several recent research works can be related to the present one, considering « true » shape optimisation problems with deformable boundaries, or inverse problems where the position and shape of an unknown boundary are sought.
Some of these works consider the case where the underlying differential operator is elliptic, for example the Bernoulli Problem (see [3], [9], [11], [14], [15]). For this problem, we look for the position of an unknown boundary of the domain so that the solution of the PDE satisfies some over-determined boundary conditions on the known part of the boundary.
There are also many works considering the Stokes or the Navier-Stokes problem in the view to optimise some quantities related to the flows (see for example [19] or [2] where the authors study the dependence of the drag with respect to the variation of the domain), or to solve some free boundary problems or inverse problems (see [1], where the author try to detect the position of an interior boundary by measuring some data on the known boundary).
In our problem, we consider an original situation with mixed boundary conditions on the fixed (outer) part of the domain. Moreover, since our obstacles are supposed to be rigid, we adapted the general shape optimisation techniques in the following way : we first consider general deformation vector fields, and then impose these vector fields to be constant on the obstacles.
For practical reasons, we use the two-dimensional case although all the calculations can be carried out in the three-dimensional case.

The paper is organised as follows : the problem is described in Section 2 and the notations are given there, the Section 3 is devoted to the existence and uniqueness of the solution of the Stokes problem in a given geometry and then the calculations and mathematical results about the derivation of the domain are given in Section 4. In section 5 we describe the iterative numerical method that is successfully tested in Section 6.
We mention that the calculations are detailed for the case of spherical obstacles, for which only translations need to be considered. We then briefly explain how the method can be adapted to non-spherical obstacles, for which we also need to consider rotations, and show his efficiency in the numerical Section.

## 2 Fluid flow with imposed constraint

Consider a bounded domain $\mathcal{D} \subset \mathbb{R}^2$ where the boundary $\partial\mathcal{D}$ is composed of three distinct parts : the inlet $\Gamma_{\text{in}}$, the outlet $\Gamma_{\text{out}}$ and the lateral boundaries $\Gamma$. Inside $\mathcal{D}$, we place obstacles described by an open set $B$ (not necessarily connected ; we can think of a collection of $N$ disjoint balls) ensuring that $\Omega = \mathcal{D} \setminus \overline{B}$ is connected. A typical configuration is that shown on Figure 1, which will be studied more precisely in the Section 6 devoted to numerical applications.

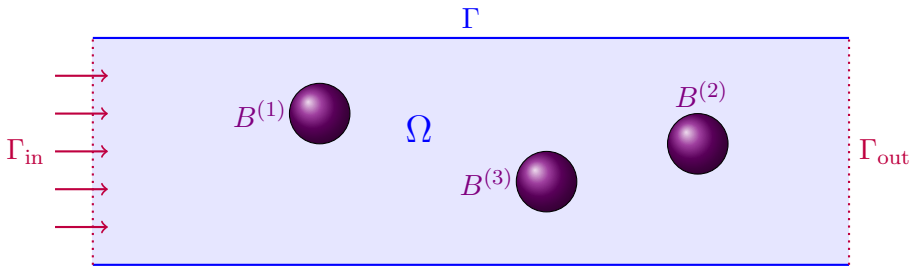


FIGURE 1 – Configuration where the obstacle $B$ is composed of 3 disjoint balls : $B = \bigcup_{i=1}^{3} B^{(i)}$.

About the regularity of the domains involved, we assume that there exists $s \geq 0$ such that

$$\text{the boundary components } \Gamma,\ \Gamma_{\text{in}},\ \Gamma_{\text{out}} \text{ and } \partial B \text{ are of class } \mathcal{C}^{s+1,1}. \tag{1}$$

We are interested in the flow of a fluid modelled by the Stokes equations in $\Omega$ :

$$\begin{cases} \text{div } \mathbf{u} = 0 & & \text{in } \Omega \\ \text{div } \boldsymbol{\sigma} = 0 \quad \text{where} \quad \boldsymbol{\sigma} = -p\,\mathbf{Id} + 2\mu\mathbf{Du} & & \text{in } \Omega \\ \mathbf{u} = \mathbf{0} & & \text{on } \Gamma \cup \partial B \\ \boldsymbol{\sigma} \cdot \mathbf{n} = -F\mathbf{n} & & \text{on } \Gamma_{\text{in}} \\ \boldsymbol{\sigma} \cdot \mathbf{n} = \mathbf{0} & & \text{on } \Gamma_{\text{out}} \end{cases} \tag{2}$$

The unknowns are the velocity field $\mathbf{u} : \Omega \longrightarrow \mathbb{R}^n$ and the pressure field $p : \Omega \longrightarrow \mathbb{R}$. The stress field $\boldsymbol{\sigma} : \Omega \longrightarrow \mathbb{R}^{n\times n}$ being explicitly given with respect to these quantities. The data are the viscosity of the medium noted $\mu > 0$ as well as the force imposed at the input $F > 0$. The vector $\mathbf{n}$ introduced in this formulation corresponds to the outgoing unit normal to $\Omega$. It is defined almost everywhere on the boundaries as soon as $\Omega$ is piecewise $\mathcal{C}^1$ regular, which will be assumed hereafter. Finally, the notation $\mathbf{Du}$ designates the symmetrical part of the velocity gradient $\nabla\mathbf{u}$ and corresponds, in physical terms, to the rate of deformation.

The quantity to be optimised is the flow rate through the domain. This can be defined by

$$\mathcal{Q} = -\int_{\Gamma_{\text{in}}} \mathbf{u}\cdot\mathbf{n}. \tag{3}$$

**Remark 1** *The incompressibility condition div* $\mathbf{u} = 0$ *and the homogeneous boundary conditions on the lateral bound* $\Gamma$ *show that this flow rate is the same if we choose as definition*

$$\mathcal{Q} = \int_{\Gamma_{\text{out}}} \mathbf{u}\cdot\mathbf{n}. \tag{4}$$

## 3 Existence, uniqueness and regularity of flow

In the following, we use the classical notations for the Lebesgue and Sobolev spaces $L^2(\Omega)$ and $H^1(\Omega)$, and use bold fonts for the spaces of vector valued functions (such as $\mathbf{H}^1(\Omega)$).
Following the work of [10], we know that for any value of $F$, there exists a unique weak solution $(\mathbf{u}, p)$ to (2) as soon as the boundaries $\Gamma \cup \partial B$ and $\Gamma_{\text{in}} \cup \Gamma_{\text{out}}$ are non-empty.

More precisely, a weak solution is defined as a pair $(\mathbf{u}, p) \in \mathbf{H}^1(\Omega) \times L^2(\Omega)$ such that

$$\begin{cases} \text{div } \mathbf{u} = 0 & \text{in } \Omega \\ \displaystyle\int_\Omega \boldsymbol{\sigma} : \nabla\boldsymbol{\varphi} = -\int_{\Gamma_{\text{in}}} F\,\mathbf{n}\cdot\boldsymbol{\varphi} & \forall \boldsymbol{\varphi} \in \mathbf{W}(\Omega) \\ \boldsymbol{\sigma} = -p\,\mathbf{Id} + 2\mu\mathbf{D}\mathbf{u} & \text{in } \Omega \\ \mathbf{u} = \mathbf{0} & \text{on } \Gamma \cup \partial B \end{cases} \tag{5}$$

where $\mathbf{W}(\Omega) = \{\boldsymbol{\varphi} \in \mathbf{H}^1(\Omega),\ \boldsymbol{\varphi} = 0 \text{ on } \Gamma \cup \partial B\}$, and where for two 2-tensors $\mathbf{A}$ and $\mathbf{B}$, the notation $\mathbf{A} : \mathbf{B}$ corresponds to the real $\mathbf{A} : \mathbf{B} = \sum_{i,j} A_{ij}B_{ji}$.

In the following study, we will need a more regular notion of solution, for a little more general problem.

**Theorem 1** *Under the Assumption* (1)*, if* $\mathrm{e} \in H^{s+1}(\Omega)$, $\mathbf{f} \in \mathbf{H}^s(\Omega)$, $\mathbf{g} \in \mathbf{H}^{s+\frac{3}{2}}(\Gamma \cup \partial B)$ *and* $\mathbf{h} \in \mathbf{H}^{s+\frac{1}{2}}(\Gamma_{\text{in}} \cup \Gamma_{\text{out}})$ *then the unique weak solution* $(\mathbf{w}, q)$ *of the problem*

$$\begin{cases} \text{div } \mathbf{w} = \mathrm{e} & \textit{in } \Omega \\ \text{div } \boldsymbol{\tau} = \mathbf{f} \quad \textit{where} \quad \boldsymbol{\tau} = -q\,\mathbf{Id} + 2\mu\mathbf{D}\mathbf{w} & \textit{in } \Omega \\ \mathbf{w} = \mathbf{g} & \textit{on } \Gamma \cup \partial B \\ \boldsymbol{\tau}\cdot\mathbf{n} = \mathbf{h} & \textit{on } \Gamma_{\text{in}} \cup \Gamma_{\text{out}} \end{cases} \tag{6}$$

*is regular : for every subset* $\omega \Subset \overline{\Omega}$ *not containing the points of* $\overline{\Gamma} \cap (\overline{\Gamma_{\text{in}}} \cup \overline{\Gamma_{\text{out}}})$*, that is the points where the boundary condition changes, we have*

$$\mathbf{w} \in \mathbf{H}^1(\Omega) \cap \mathbf{H}^{s+2}(\omega \cap \Omega) \quad \textit{and} \quad q \in L^2(\Omega) \cap H^{s+1}(\omega \cap \Omega).$$

**Proof** :
**Step 1** - The non-zero divergence condition is raised, for example using Bogovski's operator (see [4, 6]) : there exists $\widehat{\mathbf{w}} \in \mathbf{H}^{s+2}(\Omega)$ such that div $\widehat{\mathbf{w}} = \mathbf{e}$ in $\Omega$ and $\widehat{\mathbf{w}} = \mathbf{g}$ on $\Gamma \cup \partial B$. The velocity $\overline{\mathbf{w}} = \mathbf{w} - \widehat{\mathbf{w}}$ satisfies

$$\begin{cases} \text{div } \overline{\mathbf{w}} = 0 & \text{in } \Omega \\ \text{div } \boldsymbol{\tau} = \mathbf{f} - \mu\Delta\widehat{\mathbf{w}} \quad \text{where} \quad \boldsymbol{\tau} = -p\,\mathbf{Id} + 2\mu\mathbf{D}\overline{\mathbf{w}} & \text{in } \Omega \\ \overline{\mathbf{w}} = \mathbf{0} & \text{on } \Gamma \cup \partial B \\ \boldsymbol{\tau}\cdot\mathbf{n} = \mathbf{h} - \mathbf{D}\widehat{\mathbf{w}}\cdot\mathbf{n} & \text{on } \Gamma_{\text{in}} \cup \Gamma_{\text{out}} \end{cases} \tag{7}$$

As indicated in the introduction to this section, the work of [10] indicates that this system admits a unique weak solution $(\overline{\mathbf{w}}, p) \in \mathbf{H}^1(\Omega) \times L^2(\Omega)$.

**Step 2** - The method of differential quotients due to Niremberg (see for example [16]) leads to the following interior regularity result

$$\forall \omega \Subset \Omega \qquad \overline{\mathbf{w}} \in \mathbf{H}^{s+2}(\omega) \quad \text{and} \quad p \in H^{s+1}(\omega). \tag{8}$$

Using the same method, which is based on the method of translations, we can establish the regularity of solutions at any point $\mathbf{x} \in \partial\Omega$ on which the condition imposed is either of the Dirichlet type ($\mathbf{x} \in \Gamma \cup \partial B$), or of the Neumann type ($\mathbf{x} \in \Gamma_{\text{in}} \cup \Gamma_{\text{out}}$).

**Note** - On the other hand, for any point $\mathbf{x} \in \overline{\Gamma} \cap (\overline{\Gamma_{\text{in}}} \cup \overline{\Gamma_{\text{out}}})$, the technique used is inoperative since the method of translations does not give sufficient information. We even know that the solution of such a problem can be irregular at these points (for more details, see [17]). □

Applying the Theorem 1 with $\mathrm{e} = 0$, $\mathbf{f} = \mathbf{0}$, $\mathbf{g} = \mathbf{0}$ and $\mathbf{h} = -F\mathbf{n}\mathbb{1}_{\Gamma_{\text{in}}}$ we deduce the following result :

**Corollary 1** *Under the Assumption* (1), *there exists a unique solution* $(\mathbf{u}, p)$ *to* (2) *such that*

$$\forall \omega \Subset \Omega \qquad \mathbf{u} \in \mathbf{H}^1(\Omega) \cap \mathbf{H}^{s+2}(\omega \cap \Omega) \quad \textit{and} \quad p \in L^2(\Omega) \cap H^{s+1}(\omega \cap \Omega).$$

## 4 Dependence of the solution with respect to the obstacle

In order to determine the dependence of this solution with respect to the obstacle, we will slightly perturb this system using a vector field chosen from the following set :

$$\mathcal{S} = \left\{ \mathbf{v} \in \mathcal{C}^\infty(\mathcal{D}, \mathbb{R}^2) \ ; \ \mathrm{Supp}(\mathbf{v}) \subset \mathcal{D} \right\}.$$

Thus, given $\mathbf{v} \in \mathcal{S}$, for $t \in \mathbb{R}$ sufficiently small, the transformation $\mathbf{F}_t = \mathbf{id} + t\mathbf{v}$ is a diffeomorphism of $\mathcal{D}$ onto itself. For such values of $t$, we note $\Omega_t = \mathbf{F}_t(\Omega)$ and $B_t = \mathbf{F}_t(B)$, see the Figure 2.

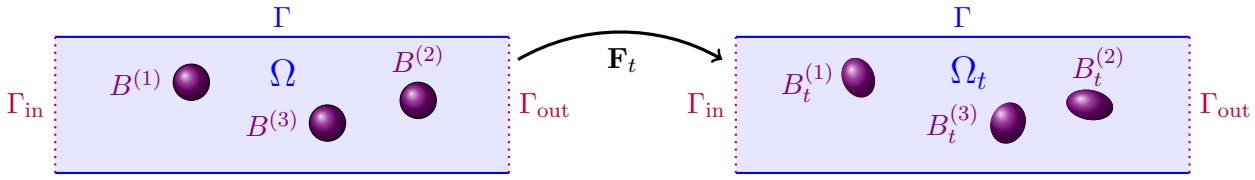


FIGURE 2 – Effect of the deformation $\mathbf{F}_t$ on the domain $\Omega$.

**Remark 2** *The only constraints we will impose on the vector fields* $\mathbf{v} \in \mathcal{S}$ *used hereafter are that they must be constant over each connected component of the obstacle, see the Section 5.1. It is therefore sufficient to work with regular vector fields. On the other hand, if we had worked with deformable obstacles, the regularity of* $\mathbf{v}$ *would have been linked to that of the obstacles.*

The theorem 1 applies to the problem (2) defined in $\Omega_t$. More precisely, we denote $(\mathbf{u}_t, p_t)$ the solution of the following problem :

$$\begin{cases} \operatorname{div} \mathbf{u}_t = 0 & & \text{in } \Omega_t \\ \operatorname{div} \boldsymbol{\sigma}_t = 0 \quad \text{where} & \boldsymbol{\sigma}_t = -p_t\,\mathbf{Id} + 2\mu\mathbf{D}\mathbf{u}_t & \text{in } \Omega_t \\ \mathbf{u}_t = \mathbf{0} & & \text{on } \Gamma \cup \partial B_t \\ \boldsymbol{\sigma}_t \cdot \mathbf{n} = -F\mathbf{n} & & \text{on } \Gamma_{\text{in}} \\ \boldsymbol{\sigma}_t \cdot \mathbf{n} = \mathbf{0} & & \text{on } \Gamma_{\text{out}} \end{cases} \tag{9}$$

The idea is to compare the solution $(\mathbf{u}, p)$ of the system (2) with the solution $(\mathbf{u}_t, p_t)$ of the system (9) when $t$ is small, and more precisely to calculate the following Eulerian derivatives :

$$\mathbf{u}'(\Omega, \mathbf{v}) = \lim_{t\to 0} \frac{\mathbf{u}_t - \mathbf{u}}{t} \qquad \text{and} \qquad p'(\Omega, \mathbf{v}) = \lim_{t\to 0} \frac{p_t - p}{t}. \tag{10}$$

These limits (more simply noted $\mathbf{u}'$ and $p'$) are not immediately evaluable since they involve two quantities, for example $\mathbf{u}_t$ and $\mathbf{u}$ for velocity, which are not defined on the same set (on $\Omega_t$ for the first and on $\Omega$ for the second). Initially, we will use the change of variable $\mathbf{F}_t : \Omega \longrightarrow \Omega_t$ and note, for all $\mathbf{x} \in \Omega$ :

$$\mathbf{u}^t(\mathbf{x}) = \mathbf{u}_t(\mathbf{F}_t(\mathbf{x})) \qquad \text{and} \qquad p^t(\mathbf{x}) = p_t(\mathbf{F}_t(\mathbf{x})). \tag{11}$$

With this change of variable, the system (9) is rewritten

$$\begin{cases} \mathbf{A}_t : \nabla \mathbf{u}^t = 0 & \text{in } \Omega \\ \mathbf{A}_t : \nabla \boldsymbol{\sigma}^t = \mathbf{0} \quad \text{where} \quad \boldsymbol{\sigma}^t = -p^t\,\mathbf{Id} + \mu(\mathbf{A}_t \cdot \nabla \mathbf{u}^t + (\nabla \mathbf{u}^t)^\intercal \cdot (\mathbf{A}_t)^\intercal) & \text{in } \Omega \\ \mathbf{u}^t = \mathbf{0} & \text{on } \Gamma \cup \partial B \\ \boldsymbol{\sigma}^t \cdot \mathbf{n} = -F\mathbf{n} & \text{on } \Gamma_{\text{in}} \\ \boldsymbol{\sigma}^t \cdot \mathbf{n} = \mathbf{0} & \text{on } \Gamma_{\text{out}} \end{cases} \tag{12}$$

where we have introduced the Jacobian matrix $\mathbf{A}_t = (\nabla \mathbf{F}_t)^{-1}$. Note that when $\mathbf{A}$ is a 2-tensor and $\mathbf{B}$ is a 3-tensor (like $\nabla \boldsymbol{\sigma}^t$ here), the notation $\mathbf{A} : \mathbf{B}$ corresponds to the vector whose the coordinates are $(\mathbf{A} : \mathbf{B})_k = \sum_{i,j} A_{ij} B_{jik}$.

**Proposition 1** *For small values of $t$, the application $t \longmapsto (\mathbf{u}^t, p^t)$ is regular.*

**Proof** :
The proof uses the ideas as the proof of Theorem 4.2 in [5], adapted to the regular solutions.
Let $(\mathbf{u}, p)$ be the regular solution of the system (2) (see the Corollary 1), and consider the mapping

$$\begin{array}{rccl} \mathcal{H} \ : \ I \times E & \longrightarrow & H^{s+1}(\Omega) \times \mathbf{H}^s(\Omega) \\ (t, (\mathbf{w}, q)) & \longmapsto & (\mathbf{A}_t : \nabla(\mathbf{w} + \mathbf{u}), \mathbf{A}_t : \nabla \boldsymbol{\tau}(\mathbf{u} + \mathbf{w}, p + q)) \end{array}$$

where $\boldsymbol{\tau}(\mathbf{w}, q) = -q\,\mathbf{Id} + \mu(\mathbf{A}_t \cdot \nabla \mathbf{w} + (\nabla \mathbf{w})^\intercal \cdot (\mathbf{A}_t)^\intercal)$, $I$ is an open interval of $\mathbb{R}$ containing 0, that we will choose during the proof, and $E$ the following functional space

$$E = \Big\{ (\mathbf{w}, q) \in \mathbf{H}^1(\Omega) \times L^2(\Omega) \ ; \ \forall \omega \Subset \Omega \quad (\mathbf{w}, q) \in \mathbf{H}^{s+2}(\omega) \times H^{s+1}(\omega) \\ \mathbf{w} = \mathbf{0} \quad \text{on } \Gamma \cup \partial B \quad \text{and} \quad \boldsymbol{\tau}(\mathbf{w}, q) \cdot \mathbf{n} = \mathbf{0} \quad \text{on } \Gamma_{\text{in}} \cup \Gamma_{\text{out}} \Big\}.$$

Note that $(\mathbf{u}^t, p^t)$ is solution of (12) is equivalent to $\mathcal{H}(t, (\mathbf{u}^t - \mathbf{u}, p^t - p)) = (0, \mathbf{0})$. The aim is to apply the implicit function theorem to this function $\mathcal{H}$ in the neighbourhood of $t = 0$.

**Step 1** - The function $\mathcal{H}$ is clearly well defined and with values in $H^{s+1}(\Omega) \times \mathbf{H}^s(\Omega)$. It is regular since $t \longmapsto \mathbf{A}_t = (\mathrm{Id} + t\nabla \mathbf{v})^{-1}$ is regular (for $t$ small enough) and since the function $\mathcal{H}$ is affine with respect to the variables $\mathbf{w}$ and $q$.

**Step 2** - For $t = 0$, by definition of the regular solution $(\mathbf{u}, p)$ of (2), we have $\mathcal{H}(0, (\mathbf{0}, 0)) = (0, \mathbf{0})$.

**Step 3** - Using the fact that $\mathcal{H}$ is affine with respect to the variables $\mathbf{w}$ and $q$, it is easy to evaluate its differential with respect to these variables :

$$\begin{array}{rccl} d_{(\mathbf{w},q)}\mathcal{H}(t, (\mathbf{w}, q)) \ : \ E & \longrightarrow & H^{s+1} \times \mathbf{H}^s(\Omega) \\ (\delta\mathbf{w}, \delta q) & \longmapsto & (\mathbf{A}_t : \nabla(\delta\mathbf{w}), \mathbf{A}_t : \nabla \boldsymbol{\tau}(\delta\mathbf{w}, \delta q)) \end{array}$$

The theorem 1, used in the case $\mathbf{g} = \mathbf{0}$ and $\mathbf{h} = \mathbf{0}$, exactly indicates that the application $d_{(\mathbf{w},q)}\mathcal{H}(0,(\mathbf{0},0))$ is invertible.

**Conclusion** - Invoking the implicit function theorem, we deduce that in the neighbourhood of $t = 0$, $\mathbf{u}^t = \mathbf{u}$ and $p^t = p$ there exists a regular function $\varphi : I \longmapsto E$ such that

$$\mathcal{H}(t,(\mathbf{u}^t - \mathbf{u}, p^t - p)) = (0,\mathbf{0}) \quad \Longleftrightarrow \quad (\mathbf{u}^t, p^t) = \varphi(t),$$

which corresponds to the announced result. □

To determine the derivatives of this application at $t = 0$, we derive the system (12) with respect to $t$ and then evaluate it at $t = 0$. Since $\nabla \mathbf{F}_t = \mathbf{Id} + t\nabla\mathbf{v}$, we use the following Taylor expansion :

$$\mathbf{A}_t = \mathbf{Id} - t\,\nabla\mathbf{v} + \mathcal{O}(t^2). \tag{13}$$

We deduce, denoting $\dot{\mathbf{u}} = \partial_t(\mathbf{u}^t)|_{t=0}$ (with the same notations for the pressure $p$ and the stress $\boldsymbol{\sigma}$) :

$$\begin{cases} -\nabla\mathbf{v} : \nabla\mathbf{u} + \operatorname{div}\dot{\mathbf{u}} = 0 & \text{in } \Omega \\ -\nabla\mathbf{v} : \nabla\boldsymbol{\sigma} + \operatorname{div}\dot{\boldsymbol{\sigma}} = 0 & \\ \quad \text{where} \quad \dot{\boldsymbol{\sigma}} = -\dot{p}\,\mathbf{Id} + 2\mu\mathbf{D}\dot{\mathbf{u}} - \mu(\nabla\mathbf{v}\cdot\nabla\mathbf{u} + (\nabla\mathbf{u})^\intercal\cdot(\nabla\mathbf{v})^\intercal) & \text{in } \Omega \\ \dot{\mathbf{u}} = \mathbf{0} & \text{on } \Gamma \cup \partial B \\ \dot{\boldsymbol{\sigma}}\cdot\mathbf{n} = \mathbf{0} & \text{on } \Gamma_{\text{in}} \\ \dot{\boldsymbol{\sigma}}\cdot\mathbf{n} = \mathbf{0} & \text{on } \Gamma_{\text{out}} \end{cases} \tag{14}$$

In order to make the link with the Eulerian derivative of $\mathbf{u}^t$, i.e. $\mathbf{u}'$, see the definition (10), we derive with respect to $t$ the relations (11). Using the fact that $\mathbf{F}_t = \mathbf{id} + t\mathbf{v}$, we also have (we write it for $\mathbf{u}$ but we have similar relation for $p$) :

$$\partial_t\mathbf{u}^t(x) = (\partial_t\mathbf{u}_t)(\mathbf{F}_t(x)) + \mathbf{v}(x)\cdot(\nabla\mathbf{u}_t)(\mathbf{F}_t(x)). \tag{15}$$

Thus, evaluating for $t = 0$, we deduce

$$\dot{\mathbf{u}} = \mathbf{u}' + \mathbf{v}\cdot\nabla\mathbf{u}. \tag{16}$$

The system (14) can then be rewritten as a system of unknowns $(\mathbf{u}', p')$ :

**Proposition 2** *The derivative $(\mathbf{u}', p')$ is the solution of*

$$\begin{cases} \operatorname{div}\mathbf{u}' = 0 & \textit{in } \Omega \\ \operatorname{div}\boldsymbol{\sigma}' = 0 \quad \textit{where} \quad \boldsymbol{\sigma}' = -p'\,\mathbf{Id} + 2\mu\mathbf{D}\mathbf{u}' & \textit{in } \Omega \\ \mathbf{u}' = -\mathbf{v}\cdot\nabla\mathbf{u} & \textit{on } \Gamma \cup \partial B \\ \boldsymbol{\sigma}'\cdot\mathbf{n} = \mathbf{0} & \textit{on } \Gamma_{\text{in}} \\ \boldsymbol{\sigma}'\cdot\mathbf{n} = \mathbf{0} & \textit{on } \Gamma_{\text{out}} \end{cases} \tag{17}$$

**Remark 3** *According to the definition of shape derivatives, see definition* (10)*, the derivatives depend on the vector field* $\mathbf{v}$*. In practice, Proposition 2 indicates that these derivatives depend only on the value of the vector field* $\mathbf{v}$ *on the boundaries of the obstacle* $\partial B$ *(*$\mathbf{v}$ *always being zero on* $\Gamma$*).*

**Proposition 3** *Under the assumption* (1)*, the problem* (17) *admits a unique solution* $(\mathbf{u}', p')$ *such that*

$$\forall\omega \Subset \mathcal{D} \qquad \mathbf{u}' \in \mathbf{H}^1(\Omega)\cap\mathbf{H}^{s+1}(\omega\cap\Omega) \quad \textit{and} \quad p' \in L^2(\Omega)\cap H^s(\omega\cap\Omega). \tag{18}$$

**Proof** : We apply the Theorem 1 with $\mathrm{e} = 0$, $\mathbf{f} = \mathbf{0}$, $\mathbf{g} = -\mathbf{v}\cdot\nabla\mathbf{u}$ and $\mathbf{h} = \mathbf{0}$. All we need to know is the regularity of $\mathbf{v}\cdot\nabla\mathbf{u}$ on $\Gamma\cap\partial B$ :
From Corollary 1 we know that the velocity field $\mathbf{u}$ arising from the problem (2) has regularity $\mathbf{H}^{s+2}$, except close to the boundary $\partial\mathcal{D}$. Since $\mathrm{Supp}(\mathbf{v}) \subset \mathcal{D}$, we therefore know that $\mathbf{v}\cdot\nabla\mathbf{u} \in \mathbf{H}^{s+1}(\omega)$ where $\omega$ is a neighbourhood of $B$. A trace theorem implies that $\mathbf{v}\cdot\nabla\mathbf{u} \in \mathbf{H}^{s+\frac{1}{2}}(\Gamma\cap\partial B)$. □

# 5 Optimising the position of the obstacles

In this section, we will use the previous theoretical results to set up a numerical method for optimising the flow rate $\mathcal{Q}$ through $\Omega$ according to the position of rigid spherical obstacles.
We assume that the obstacle $B$ is made up of a family of $N$ disjoint balls of the same radius $R > 0$ (this assumption can also easily be omitted and we could consider balls of different radii, or non-spherical obstacles, see the subsection 5.2 for examples) :

$$B = \bigcup_{i=1}^{N} B^{(i)} \quad \text{where } B^{(i)} = B(\mathbf{x}^{(i)}, R).$$

To ensure that the balls are disjoint and all included in $\mathcal{D}$, we must assume that their centers satisfy certain constraints. More precisely, let $\mathcal{D}_R^N$ be the open set defined by

$$\begin{aligned} \mathcal{D}_R^N = \big\{ \mathbf{X} = (\mathbf{x}^{(1)}, ..., \mathbf{x}^{(N)}) \in \mathcal{D}^N \subset \mathbb{R}^{2N} \ ; \\ \forall i \in \{1, ..., N\} \quad \text{dist}(\mathbf{x}^{(i)}, \partial\mathcal{D}) > R \quad \text{and} \\ \forall (i,j) \in \{1, ..., N\}^2 \quad i \neq j \Longrightarrow \text{dist}(\mathbf{x}^{(i)}, \mathbf{x}^{(j)}) > 2R \big\}, \end{aligned} \tag{19}$$

the objective is to find a position $\mathbf{X} \in \mathcal{D}_R^N$ so that the flow $\mathcal{Q}$ resulting from the calculation of the Stokes problem is optimal. We can write the flow rate as a function of the positions of the $N$ centers :

$$\begin{array}{rccc} \mathcal{Q} & : & \mathcal{D}_R^N & \longrightarrow & \mathbb{R} \\ & & \mathbf{X} & \longmapsto & -\displaystyle\int_{\Gamma_{\text{in}}} \mathbf{u} \cdot \mathbf{n}. \end{array} \tag{20}$$

and the question is then to determine $\mathbf{X}_\star \in \mathcal{D}_R^N$ such that

$$\mathcal{Q}(\mathbf{X}_\star) = \min_{\mathbf{X} \in \mathcal{D}_R^N} \mathcal{Q}(\mathbf{X}). \tag{21}$$

**Remark 4** *Since the set $\mathcal{D}_R^N$ is not a compact set, it is not clear that the minimum is reached. From a numerical point of view, the constraints imposed in $\mathcal{D}_R^N$ will be imposed to the nearest mesh $\delta x$. Thus* $\text{dist}(\mathbf{x}^{(i)}, \partial\mathcal{D}) > R$ *will be written as* $\text{dist}(\mathbf{x}^{(i)}, \partial\mathcal{D}) \geq R + \delta x$ *and* $\text{dist}(\mathbf{x}^{(i)}, \mathbf{x}^{(j)}) > 2R$ *will be written as* $\text{dist}(\mathbf{x}^{(i)}, \mathbf{x}^{(j)}) \geq 2R + \delta x$. *In this context, at a fixed $\delta x$, at least one minimum will exist and the aim of the following section is to propose an algorithm for approaching such a minimum.*

## 5.1 Numerical approach

The aim of this section is to explain who to use the previous calculations to set up a descent algorithm, that is how to build a sequence $(\mathbf{X}_k)_{k \in \mathbb{N}}$ of elements of $\mathcal{D}_R^N$ such that the values of $\mathcal{Q}(\mathbf{X})_k$ decrease. More precisely, the iteration is written as follows

$$\mathbf{X}_{k+1} = \mathbf{X}_k + \alpha_k \mathbf{v}_k. \tag{22}$$

In order to approach a minimum for the function $\mathcal{Q}$, the Taylor expansion

$$\mathcal{Q}(\mathbf{X}_k + \alpha_k \mathbf{v}_k) = \mathcal{Q}(\mathbf{X}_k) + \alpha_k \partial_{\mathbf{v}_k} \mathcal{Q}(\mathbf{X}_k) + \frac{1}{2} \alpha_k^2 \partial_{\mathbf{v}_k}^2 \mathcal{Q}(\mathbf{X}_k) + \mathcal{O}(\alpha_k^3) \tag{23}$$

indicates that we can choose

$$\mathbf{v}_k \quad \text{such that} \quad \partial_{\mathbf{v}_k} \mathcal{Q}(\mathbf{X}_k) \leq 0.$$

We then choose the descent step $\alpha_k$ in order to minimize the polynomial of degree 2 given by $\alpha \mapsto \mathcal{Q}(\mathbf{X}_k) + \alpha \partial_{\mathbf{v}_k} \mathcal{Q}(\mathbf{X}_k) + \frac{1}{2}\alpha^2 \partial^2_{\mathbf{v}_k} \mathcal{Q}(\mathbf{X}_k)$. We obtain the following theoretical expression :

$$\alpha_k = \frac{-\partial_{\mathbf{v}_k} \mathcal{Q}(\mathbf{X}_k)}{\partial^2_{\mathbf{v}_k} \mathcal{Q}(\mathbf{X}_k)}. \tag{24}$$

**Remark 5** *As explained in remark 4, from a theoretical point of view we do not know how to justify the existence of a unique minimum. We do not even know if the sequence* $(\mathbf{X}_k)$ *thus constructed remains in* $\mathcal{D}_R^N$*, nor if the proposed algorithm can be implemented (for example if* $\partial^2_{\mathbf{v}_k} \mathcal{Q}(\mathbf{X}_k) = 0$*). This is partly due to the fact that the functional* $\mathcal{Q}$ *is not convex. Nevertheless, we will see from the examples that the descent method is efficient and provides local minima.*

The continuation of this part consists of explaining how to explicitly evaluate the direction of descent $\mathbf{v}_k$ as well as the descent step $\alpha_k$.

**Directional derivatives of $\mathcal{Q}$** it is possible to establish a link between the directional derivative $\partial_{\mathbf{v}} \mathcal{Q}$ according to a vector $\mathbf{v} \in \mathbb{R}^{2N}$ and the derivative of form $\mathbf{u}'(\Omega, \mathbf{v})$ by a vector field $\mathbf{v} \in \mathcal{S}$ introduced by the formula (10).
In fact, each vector $\mathbf{v} \in \mathbb{R}^{2N}$ is associated with a vector field, again denoted $\mathbf{v} \in \mathcal{S}$, such that

$$\forall i \in \{1, ..., N\} \quad \forall \mathbf{x} \in B^{(i)} \quad \mathbf{v}(\mathbf{x}) = \mathbf{v}_i. \tag{25}$$

To this vector field $\mathbf{v}$, and to any parameter $t \in \mathbb{R}$ small enough, we can associate the solution $\mathbf{u}_t$ of the problem (9). From the definition of the flow $\mathcal{Q}$, we thus have

$$\frac{\mathcal{Q}(\mathbf{X} + t\mathbf{v}) - \mathcal{Q}(\mathbf{X})}{t} = -\int_{\Gamma_{\text{in}}} \frac{\mathbf{u}_t - \mathbf{u}}{t} \cdot \mathbf{n}. \tag{26}$$

From the remark 3, the shape derivative $\mathbf{u}'(\Omega, \mathbf{v})$ depends only on the values of $\mathbf{v}$ on the boundaries $\partial B^{(i)}$, $i \in \{1, ..., N\}$, and therefore only on the value of the vector $\mathbf{v} \in \mathbb{R}^{2N}$. When $t$ tends to 0, we get

$$\partial_{\mathbf{v}} \mathcal{Q}(\mathbf{X}) = -\int_{\Gamma_{\text{in}}} \mathbf{u}'(\Omega, \mathbf{v}) \cdot \mathbf{n}. \tag{27}$$

**Remark 6** *The equation* (27) *can not be used to compute the descent direction, since* $\mathbf{u}'$ *is not available and depends on* $\mathbf{v}$*. The aim of the next calculations is to get an expression which will allow us to choose* $\mathbf{v}$ *such that* $\partial_{\mathbf{v}} \mathcal{Q}$ *is negative.*

Let us now assume that the step $k$ has been completed, i.e. that we know $\mathbf{X}_k \in \mathcal{D}_R^N$.We are therefore working in the domain $\Omega_k = \mathcal{D} \setminus \overline{B_k}$ where $B_k = \cup_{i=1}^N B(\mathbf{x}_k^{(i)}, R)$ corresponds to the union of the $N$ balls centered in the $N$ pairs of the vector $\mathbf{X}_k$.

Since $\mathbf{v} \cdot \nabla \mathbf{u}$ is regular (see the proof of the proposition 3), it is possible to choose $\boldsymbol{\varphi} = \mathbf{u}' + \mathbf{v} \cdot \nabla \mathbf{u} \in \mathbf{W}(\Omega_k)$ as the test function in the weak formulation (5). We deduce

$$\underbrace{\int_{\Omega_k} \boldsymbol{\sigma} : \nabla \mathbf{u}'}_{I_1} + \underbrace{\int_{\Omega_k} \boldsymbol{\sigma} : \nabla(\mathbf{v} \cdot \nabla \mathbf{u})}_{I_2} = -\underbrace{\int_{\Gamma_{\text{in}}} F\mathbf{n} \cdot \mathbf{u}'}_{I_3} - \underbrace{\int_{\Gamma_{\text{in}}} F\mathbf{n} \cdot (\mathbf{v} \cdot \nabla \mathbf{u})}_{I_4}. \tag{28}$$

Since $\boldsymbol{\sigma} = -p\,\mathbf{Id} + 2\mu \mathbf{Du}$ and div $\mathbf{u}' = 0$, owe have

$$I_1 = \int_{\Omega_k} 2\mu \mathbf{Du} : \mathbf{Du}'. \tag{29}$$

Integrating by parts the term $I_2$, using div $\boldsymbol{\sigma} = \mathbf{0}$ and Supp $\mathbf{v} \subset \mathcal{D}$ we obtain

$$I_2 = \int_{\partial B_k} (\mathbf{v} \cdot \nabla \mathbf{u}) \cdot (\boldsymbol{\sigma} \cdot \mathbf{n}). \tag{30}$$

The contribution $I_4$ vanishes since $\mathbf{v} = \mathbf{0}$ on $\Gamma_{\text{in}}$. The equation (28) then becomes

$$\int_{\Omega_k} 2\mu \mathbf{D}\mathbf{u}' : \mathbf{D}\mathbf{u} + \int_{\partial B_k} (\mathbf{v} \cdot \nabla \mathbf{u}) \cdot (\boldsymbol{\sigma} \cdot \mathbf{n}) = -F \int_{\Gamma_{\text{in}}} \mathbf{u}' \cdot \mathbf{n}. \tag{31}$$

Similarly, taking $\mathbf{u} \in \mathbf{W}(\Omega_k)$, the solution to the equation (2), as the test function in the weak formulation of the second equation (17), we obtain

$$\int_{\Omega_k} 2\mu \mathbf{D}\mathbf{u} : \mathbf{D}\mathbf{u}' = 0. \tag{32}$$

The combination of the two relations (31) and (32) allows us to write

$$\partial_{\mathbf{v}} \mathcal{Q}(\mathbf{X}_k) = -\int_{\Gamma_{\text{in}}} \mathbf{u}' \cdot \mathbf{n} = \frac{1}{F} \int_{\partial B_k} \mathbf{v} \cdot (\nabla \mathbf{u} \cdot \boldsymbol{\sigma} \cdot \mathbf{n}). \tag{33}$$

**Remark 7** *Note that we observe that $\partial_{\mathbf{v}} \mathcal{Q}(\mathbf{X}_k)$ depends only on the normal component of $\mathbf{v}$ on $\partial B_k$, this is a consequence of the well known structure theorem of Hadamard (see for example [13]).*

Since $\partial B_k = \cup_{i=1}^N \partial B(\mathbf{x}_k^{(i)}, R)$, this quantity is negative as soon as we choose $\mathbf{v} = \mathbf{v}_k = (\mathbf{v}_k^{(1)}, ..., \mathbf{v}_k^{(N)}) \in (\mathbb{R}^2)^N$ such that for all $i \in \{1, ..., N\}$ we have

$$\mathbf{v}_k^{(i)} = -\frac{1}{F^2} \int_{\partial B(\mathbf{x}_k^{(i)}, R)} \nabla \mathbf{u} \cdot \boldsymbol{\sigma} \cdot \mathbf{n}. \tag{34}$$

**Remark 8** *The coefficient $\frac{1}{F^2}$ gives $\mathbf{v}_k$ independent of $F$, i.e. without units, and* (34) *is equivalent with :*

$$\mathbf{v}_k = -\frac{1}{F} \nabla \mathcal{Q}(\mathbf{X}_k). \tag{35}$$

*In practice, solving the problem* (2) *on $\Omega_k$ yields $\mathbf{u}$ and $\boldsymbol{\sigma}$ and therefore allows us to propose a direction of descent $\mathbf{v}_k$ defined by* (34).
*We then have :*

$$\partial_{\mathbf{v}_k} \mathcal{Q}(\mathbf{X}_k) = -\frac{1}{F} \|\nabla \mathcal{Q}(X_k)\|^2 \leq 0. \tag{36}$$

**Descent step** We first observe that the descent step must be small enough to make sure that the configuration at iteration $k+1$ is admissible, more precisely we must ensure that $\mathbf{X}_{k+1} = \mathbf{X}_k + \alpha_k \mathbf{v}_k \in \mathcal{D}_R^N$ (see (19) and Remark 4).
To do this, we compute the positive real number $M_k$ defined by :

$$M_k = \sup\{t_0 \in \mathbb{R}_+, \mathbf{X}_k + t\mathbf{v}_k \in \mathcal{D}_R^N \ \forall t \in [0, t_0]\}. \tag{37}$$

The descent step $\alpha_k$ must be chosen smaller than $M_k$. To avoid grid effects, we impose $\alpha_k \leq \frac{1}{2} M_k$.
To approximate the optimal descent step $\alpha_k$ given by (24), we need to evaluate the value of $\partial^2_{\mathbf{v}_k} \mathcal{Q}(\mathbf{X}_k)$. We would then need to compute the second order domain derivative $(\mathbf{u}'', p'')$, which is the solution of a problem similar as (17) with terms in the right hand side involving second order derivatives in space of $\mathbf{u}$ and first order derivatives in space of $\mathbf{u}'$.

These second order terms being difficult to evaluate with consistency, we turn to another approach, noting that the method suggested by (23) is actually equivalent to looking for $\alpha_k$ satisfying :

$$\partial_{\mathbf{v}_k} \mathcal{Q}(\mathbf{X}_k + \alpha_k \mathbf{v}_k) = 0, \tag{38}$$

the expression of $\alpha_k$ in (24) corresponding to the step of the Newton method to solve (38).
Thus, we first compute $\partial_{\mathbf{v}_k} \mathcal{Q}(\mathbf{X}_k)$ and $\partial_{\mathbf{v}_k} \mathcal{Q}(\mathbf{X}_k + \Lambda_k \mathbf{v}_k)$ (the choice of $\Lambda_k$ will be explained later). Looking for $\alpha_k$ satisfying (38) by linear interpolation would give $\frac{-\Lambda_k \partial_{\mathbf{v}_k} \mathcal{Q}(\mathbf{X}_k)}{\partial_{\mathbf{v}_k} \mathcal{Q}(\mathbf{X}_k + \Lambda_k \mathbf{v}_k) - \partial_{\mathbf{v}_k} \mathcal{Q}(\mathbf{X}_k)}$, thus we choose :

$$\alpha_k = \min \left( \frac{1}{2} M_k, \frac{-\Lambda_k \partial_{\mathbf{v}_k} \mathcal{Q}(\mathbf{X}_k)}{\partial_{\mathbf{v}_k} \mathcal{Q}(\mathbf{X}_k + \Lambda_k \mathbf{v}_k) - \partial_{\mathbf{v}_k} \mathcal{Q}(\mathbf{X}_k)} \right). \tag{39}$$

**Remark 9** *The expression* $\frac{-\Lambda_k \partial_{\mathbf{v}_k} \mathcal{Q}(\mathbf{X}_k)}{\partial_{\mathbf{v}_k} \mathcal{Q}(\mathbf{X}_k + \Lambda_k \mathbf{v}_k) - \partial_{\mathbf{v}_k} \mathcal{Q}(\mathbf{X}_k)}$ *for* $\Lambda_k \to 0$ *is consistent with* (24).
*Since we can not prove the convexity of the function* $\mathcal{Q}$*, we can not be sure that the value of* $\alpha_k$ *given by* (39) *is positive. Actually, we can even not be sure that* $\alpha_k$ *is defined (see also remark 5). Nevertheless, in all the numerical tests presented in the next section, we got positive values for* $\alpha_k$*.*

We now explain the choice of $\Lambda_k$ :

- For the iteration 0, we chose $\Lambda_0 = \frac{1}{2} M_0$.
- For the next iterations, we chose $\Lambda_k = \min(\frac{1}{2} M_k, \alpha_{k-1})$.

### 5.2 Non-spherical rigid obstacles

It is possible to extend the results obtained in the previous sections to the case of non-spherical obstacles. The position of each obstacle $B^{(i)}$ is characterised by the position of its center of-inertia $\mathbf{x}^{(i)} \in \mathbb{R}^2$ and by an orientation $\theta^{(i)} \in \mathbb{S}^1$. Without going into detail, we define $\mathcal{D}_S^N$ as the set of positions $\{(\mathbf{x}^{(i)}, \theta^{(i)}),\ 1 \leq i \leq N\}$ for which the obstacles $B^{(i)}$ are disjoint two by two and entirely included in $\mathcal{D}$. The flow $\mathcal{Q} : \mathcal{D}_S^N \longrightarrow \mathbb{R}$ is then seen as a function of $3N$ variables which must be minimised.

We know that a transformation of the form $\mathbf{id} + t\mathbf{v}$ does not deform a solid $B^{(i)}$ if and only if $\mathbf{Dv} = \mathbf{0}$ in $B^{(i)}$, this last property being characterised by

$$\exists \mathbf{v}_i \in \mathbb{R}^2 \quad \exists \theta_i \in \mathbb{R} \quad ; \quad \forall \mathbf{x} \in B^{(i)} \quad \mathbf{v}(\mathbf{x}) = \mathbf{v}_i + \theta_i (\mathbf{x} - \mathbf{x}^{(i)})^{\perp}.$$

Thus, to each element $(\mathbf{w}, \boldsymbol{\theta}) \in \mathcal{D}_S^N$ we can associate a vector field $\mathbf{v} \in \mathcal{S}$ such that $\mathbf{id} + t\mathbf{v}$ does not deform any solid $B^{(i)}$. This field is defined by

$$\forall i \in \{1, ..., N\} \quad \forall \mathbf{x} \in B^{(i)} \quad \mathbf{v}(\mathbf{x}) = \mathbf{w}_i + \theta_i (\mathbf{x} - \mathbf{x}^{(i)})^{\perp}, \tag{40}$$

and regularly extended outside obstacles.
From the remark 3, and using the same approach as in the previous sections (see equations (27) and (33)), we deduce that the derivative of the flow $\mathcal{Q}$ in the $(\mathbf{w}, \boldsymbol{\theta})$ direction is related to this vector field.

More precisely, at a point $\mathbf{X} \in \mathcal{D}_S^N$, we obtain the velocities $\mathbf{u}$ and stresses $\boldsymbol{\sigma}$ from the problem (2) in $\Omega = \mathcal{D} \setminus \overline{B}$. We then have

$$\begin{aligned} \partial_{(\mathbf{w}, \boldsymbol{\theta})} \mathcal{Q}(\mathbf{X}) &= \frac{1}{F} \int_{\partial B} \mathbf{v} \cdot (\nabla \mathbf{u} \cdot \boldsymbol{\sigma} \cdot \mathbf{n}) \\ &= \frac{1}{F} \sum_{i=1}^{N} \Big( \mathbf{w}_i \cdot \int_{\partial B^{(i)}} \nabla \mathbf{u} \cdot \boldsymbol{\sigma} \cdot \mathbf{n} + \theta_i \int_{\partial B^{(i)}} (\mathbf{x} - \mathbf{x}^{(i)})^{\perp} \cdot (\nabla \mathbf{u} \cdot \boldsymbol{\sigma} \cdot \mathbf{n}) \Big). \end{aligned} \tag{41}$$

In the descent method, if we want the gradient to be negative at iteration $k$, we choose $\mathbf{w}_k = (\mathbf{w}_k^{(1)}, ..., \mathbf{w}_k^{(N)}) \in (\mathbb{R}^2)^N$ and $\boldsymbol{\theta}_k = (\theta_k^{(1)}, ..., \theta_k^{(N)}) \in (\mathbb{S}^1)^N$ such that for all $i \in \{1, ..., N\}$

$$\mathbf{w}_k^{(i)} = -\frac{1}{F^2} \int_{\partial B_k^{(i)}} \nabla \mathbf{u} \cdot \boldsymbol{\sigma} \cdot \mathbf{n} \qquad \text{and} \qquad \theta_k^{(i)} = -\frac{1}{F^2 R_i} \int_{\partial B_k^{(i)}} (\mathbf{x} - \mathbf{x}_k^{(i)})^\perp \cdot (\nabla \mathbf{u} \cdot \boldsymbol{\sigma} \cdot \mathbf{n}). \tag{42}$$

where $R_i$ is the diameter of $B_k^{(i)}$. The coefficient $\frac{1}{F^2}$ has been added for the reason explained in Remark 8, and the coefficient $R_i$ in the formula defining $\theta_k^{(i)}$ has been added in order to have homogeneous coordinates in $(\mathbf{w}_k, \boldsymbol{\theta}_k)$.
The descent step is optimised in exactly the same way as for spherical obstacles.

# 6 Numerical results

We present in this section some numerical tests, showing the efficiency of the proposed method. The tests have been performed with FreeFem++ (see [12]), based on the weak formulation of the differential problem. We use P2/P1 element for the Stokes problem, with about 15000 to 20000 triangles. The mesh is refined near the obstacles, more precisely to distance between two grid points on the obstacles $\partial B$ is 10 times smaller than the distance between two grid points on the fixed part of the boundary $\partial \mathcal{D}$.
The stop criterion has been chosen in order the handle small oscillations. We then consider that the limit of the sequence $(\mathbf{X}_k)_{k \in \mathbb{N}}$ is reached for $k = k_S > 3$ satisfying :

$$\|\mathbf{X}_{k_S} - \mathbf{X}_j\| \leq \delta \tag{43}$$

for all $j \in \{k_S - 3, k_S - 2, k_S - 1\}$, where $\delta$ denoted the distance between two grid points on $\partial B$.
Before presenting numerical tests of the proposed algorithm, we present the behaviour of the function $\mathcal{Q}$ in a simple configuration.

## 6.1 A spherical obstacle in a right channel

We consider in this section a rectangular domain $\mathcal{D} = (0, 5) \times (0, 1)$ and an obstacle consisting of only one ball centered at $(x, z) : B = B^{(1)} = \{\mathbf{x} \in \mathcal{D}, \|\mathbf{x} - (x, z)\| < R\}$ of radius $R = 0.1$, where $\|.\|$ denotes here the usual Euclidean norm in $\mathbb{R}^2$, see the figure 3.

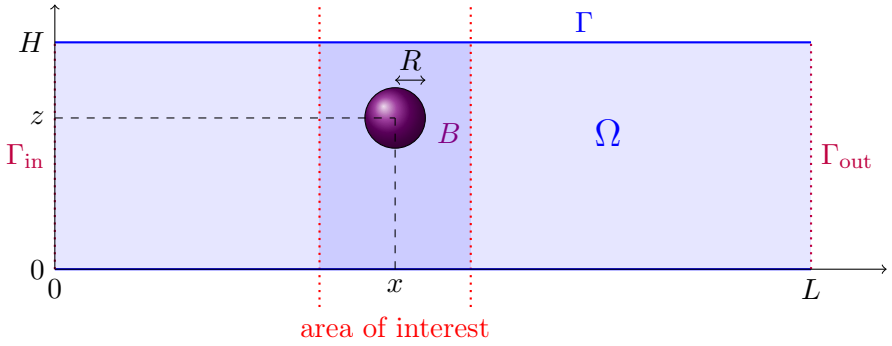


FIGURE 3 – Notations and geometric situation for one ball.

Before trying to minimise the flow $\mathcal{Q}$, it may be interesting to see how it behaves as a function of the position of the center $(x, z)$ of the ball, at least in this simple geometrical case. This is why we have made a preliminary study of two cases :

1. The location of the ball is given by $(x, z) = (2.5, z)$ with $z \in (2R, 1 - 2R)$ ;
2. The location of the ball is given by $(x, z) = (x, 0.5)$ with $x \in (2R, 5 - 2R)$.

For such configurations, we denote by $\mathcal{Q}(x, z)$ the value of the flux obtained after resolving a simple Stokes problem in $\mathcal{D} \setminus B$. The aim is to check some physical intuitions : the horizontal position $x$ of the ball has a much smaller influence on $\mathcal{Q}(x, z)$ than the horizontal position $z$.

More precisely, the dependence on the vertical variable $z$, see the figure 4 is in line with what is physically expected : the flux $\mathcal{Q}$ seems lower when the ball is at the middle of the channel and larger when the ball is close to one of the walls. Actually, the optimum solution which minimises the flow $\mathcal{Q}$ is obtained when the ball is exactly in the middle of the channel, corresponding to $z = 0.5$.

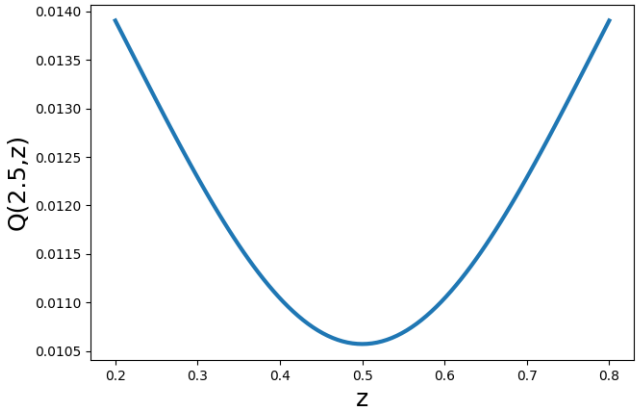


FIGURE 4 – Effect of the vertical position $z$ of the obstacle on the flow $\mathcal{Q}$.

The figure 5 shows the flux as a function of the horizontal variable $x$. There is little dependence on $x$ except when the ball is close to the boundary of the domain, i.e. when $x$ is close to 0 or close to 5. These effects, which remain relatively small, are due to the boundary conditions. Note also that the graph is not convex, which indicates that the solution will probably not always be unique.

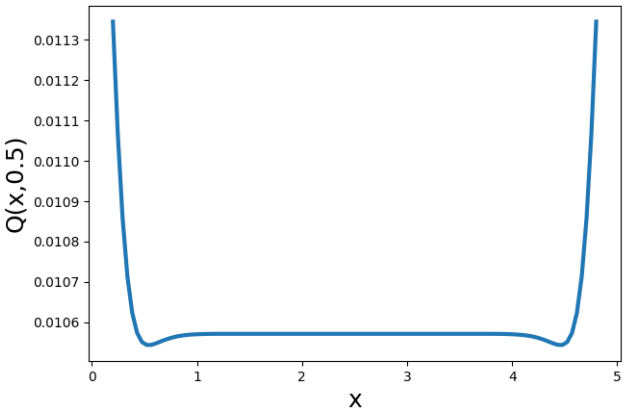


FIGURE 5 – Effect of the horizontal position $x$ of the obstacle on the flow $\mathcal{Q}$.

However, the dependence almost entirely on the variable $x$ means that we can only show what happens near the area where the ball is located. This is why, in the following figures, we will only show the zone of interest around the ball (the calculations are always carried out in the complete domain), see the so called "area of interest" introduced on figure 3.
For example, using the minimisation algorithm introduced in the previous sections, we can see (see the figure 6) how the position of the ball evolves over the iterations denoted by $k$ towards the optimum position $z = 0.5$.

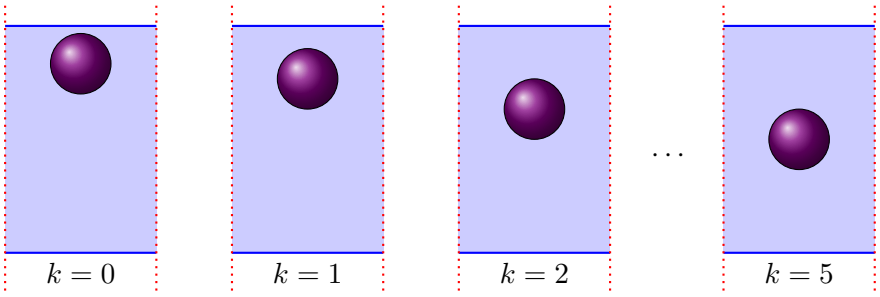


FIGURE 6 – Convergence to a position minimising the flow in the spherical case.

### 6.2 A non-spherical obstacle in a right channel

Having observed that, in the spherical case, the preferred position of the obstacle to minimise the flow was, as expected, a central position, the aim of this new test is to verify the behaviour of a non-spherical obstacle. The question of the orientation of the obstacle will therefore be interesting to understand.
In this test, we always consider the same rectangular domain $\mathcal{D} = (0, 5) \times (0, 1)$ but we assume that the obstacle $B$ is an ellipsoid of radii 0.1 and 0.05.
Starting the minimisation algorithm with the position of the center of the ellipsoid given by $(x_0, y_0) = (2.5, 0.2)$ and an angle with the horizontal direction equals to 17.1°, we observe that, as expected, the obstacle moves to the center of the tube, in an vertical direction.
In fact, the algorithm converges after 12 iterations, we present the first 6 positions, the next ones (for $k = 7$ to 12) are very close to the sixth one, see the figure 7. The value $y_k = 0.50$ obtained for $k \geq 4$ indicates that the we use the round-off with 2 digits, that is $0.495 < y_k < 0.505$. We add to these results that we got $\theta_k \in (89.55°, 90.45°)$ for $k \in \{9, 10, 11, 12\}$.

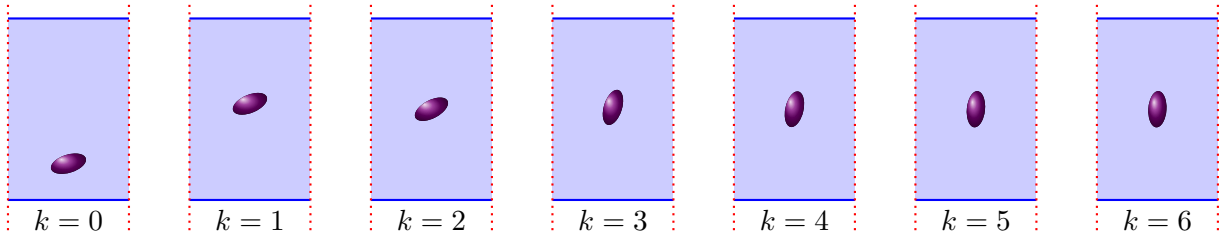


FIGURE 7 – Convergence to a minimising position in the non-spherical case.

### 6.3 Several obstacles in a right channel

The purpose of this section is to see how several obstacles are organised to minimise the flow.
As in section 6.1, we take again $\mathcal{D} = (0, 5) \times (0, 1)$ but we consider eight obstacles whose geometries and positions are described in Figure 8 (see $k = 0$).
Over the iterations, we observed the formation of clusters which seem to be independent since they are quite far one from each other. It is interesting to state that the obstacle on the right joined the three closer ones. On the left part, one obstacle remains isolated since it was to far from the left cluster at the beginning of the test. We can guess that the local minimum reached at the final state does not correspond to a global minimum, since the flow rate would be much smaller if we put the eight obstacle in one only cluster.

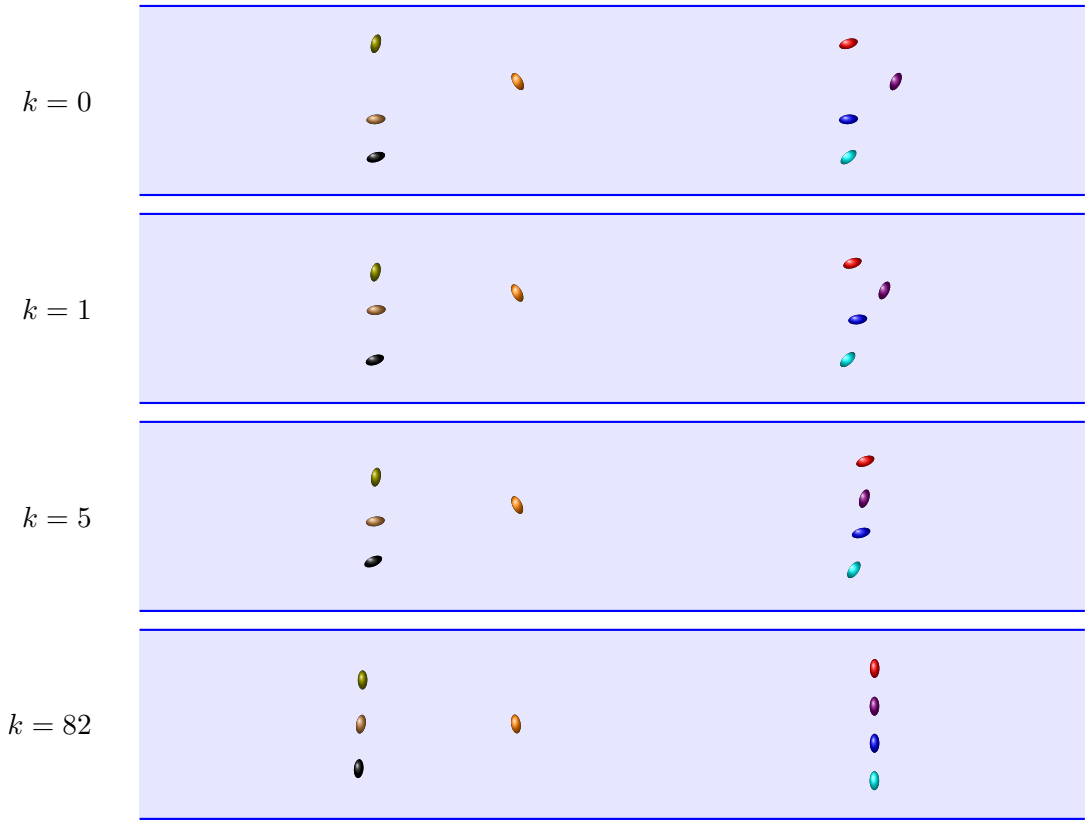


FIGURE 8 – Convergence to a minimising position for several obstacles.

### 6.4 A non-spherical obstacles in a non-right channel

In this section, we propose a test to determine the optimum position of an obstacle in a convergent-divergent channel. The domain $\mathcal{D}$ is no longer a rectangle but is given by the figure 9 (see the top figure $k = 0$ corresponding to the initial position in the algorithm).
Once again, we observe that the algorithm converges towards the solution that seems to be expected from a physical point of view : the obstacle minimises the flow as soon as it is placed at the thinnest point of the flow, and in a vertical position, see figure 9 and the converged solution obtained after 37 iterations.

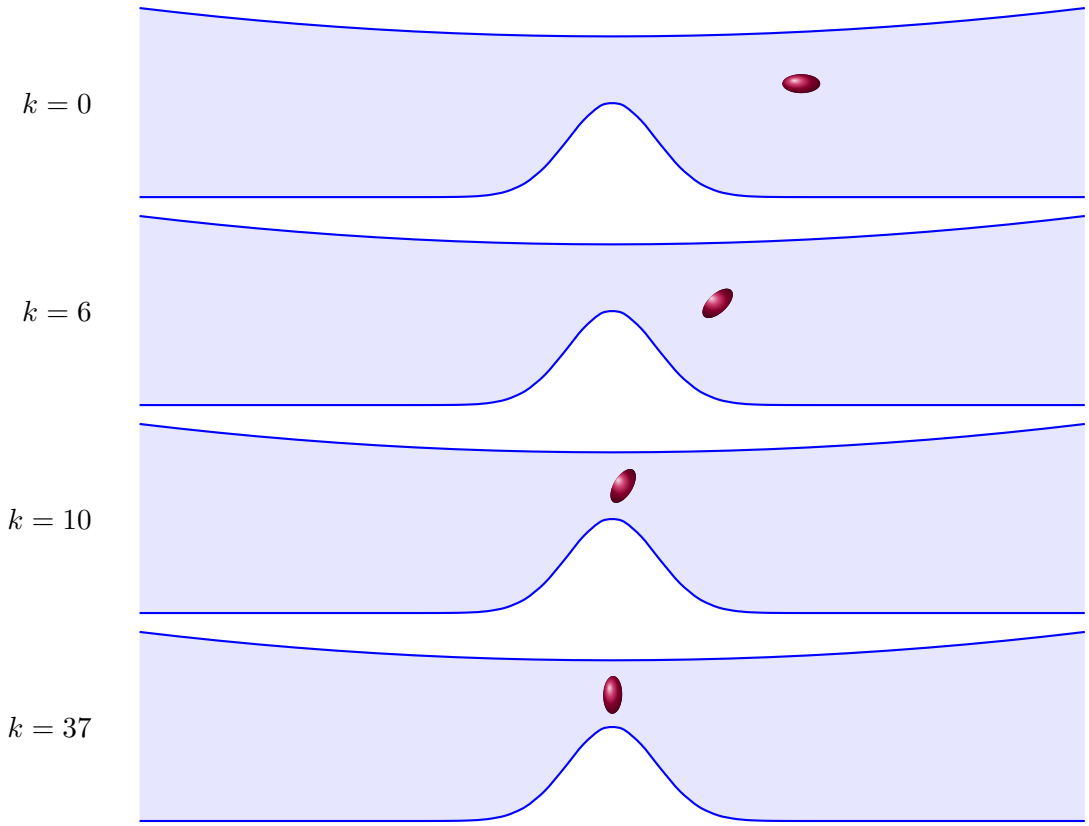


FIGURE 9 – Convergence to a minimising position of an obstacle in a convergent-divergent channel.

### 6.5 Several non-spherical obstacles in a non-right channel

In this last test, we are trying to determine the optimum position of two obstacles in a curved channel.
This configuration combines all the difficulties that can be found in this type of problem : non-rectilinear domain with no particular invariance, several obstacles that have to self-organise, non-spherical shape of the obstacles that have to orientate themselves correctly.
In the end, the optimal configuration obtained seems consistent with what might be expected : the two obstacles try to obstruct the channel as much as possible, see the figure 10.

Note that the figures show only the curved part of the domain, but to avoid edge effects, the channel in which the simulations were carried out is longer on the left and at the bottom.

## 7 Conclusion and perspectives

In this article, we studied the effect of the position of rigid obstacles in a flow. Indeed, if a flow through a domain is imposed by a constraint at the entrance to the domain, its rate depends essentially on the geometry and therefore on any obstacles.
Initially, we modelled the problem and showed that it is well posed whatever the position of the obstacles. Secondly, we studied the dependence of the solution on the position of the obstacles. Thanks to this study, we were able to set up a minimisation algorithm that determines how to place the obstacles in order to minimise the flow rate. Note in particular that we are dealing with

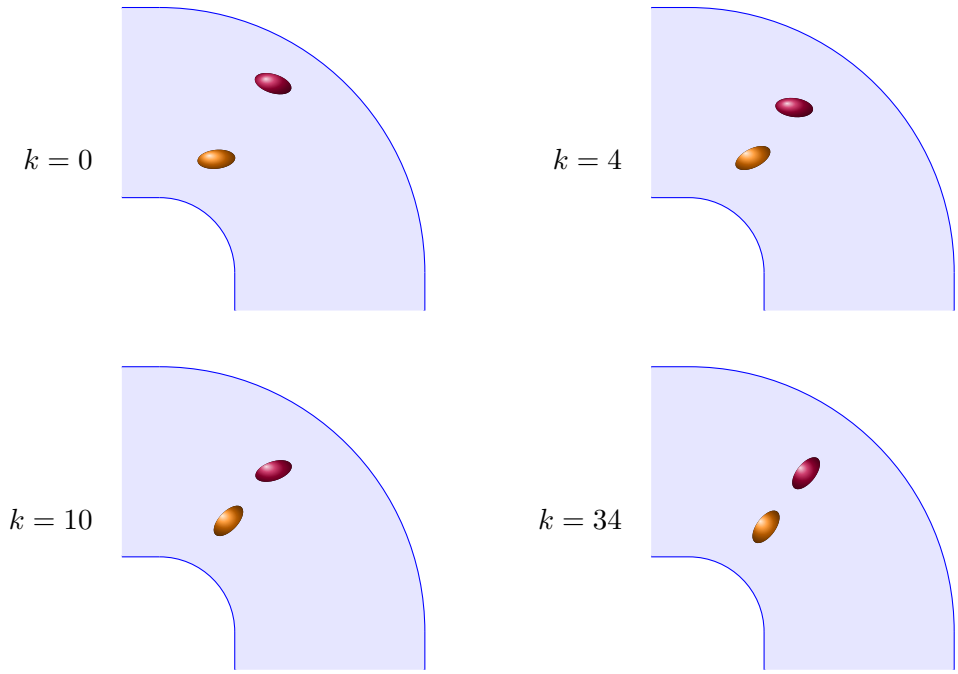


FIGURE 10 – Convergence to a minimising position of two obstacles in curved channel.

both spherical obstacles (for which the position of the centers must be optimised) and non-spherical obstacles, for which the angles must also be optimised. Finally, we carried out numerical simulations to validate our study and visualise the results. Although most of the simulations confirm intuitive results (to minimise the flow, the obstacle must be in the middle of the domain and oriented in the direction transverse to the flow), this work can provide ideas for more complex situations.
On the other hand, we can imagine extensions of this work, such as taking an interest in non-laminar flows by taking into account inertial effects (and therefore the Navier-Stokes model instead of the Stokes model), non-Newtonian flows with various rheologies, etc. With a view to applications, it could also be interesting to understand what happens when the number of obstacles is very large, each of which is small. The role of clustering will probably be important, as we have already seen in simulations with height obstacles.

## Références

[1] M. Badra, F. Caubet, and M. Dambrine. Detecting an obstacle immersed in a fluid by shape optimization methods. *Mathematical Models and Methods in Applied Sciences*, 21(10) :2069–2101, 2011.

[2] J. Bello, E. Fernández-Cara, J. Lemoine, and J. Simon. The differentiability of the drag with respect to the variations of a lipschitz domain in a navier-stokes flow. *SIAM Journal of Control and Optimization*, 35(2) :626–640, 1997.

[3] A. Ben Abda, F. Bouchon, G.H. Peichl, M. Sayeh, and R. Touzani. A dirichlet-neumann cost functional approach for the bernoulli problem. *Journal of Engineering Mathematics*, 81 :157–176, 2013.

[4] M.E. Bogovskii. Solution of the first boundary value problem for the equation of continuity of an incompressible medium. In *Doklady Akademii Nauk*, volume 248, pages 1037–1040. Russian Academy of Sciences, 1979.

[5] F. Bouchon, G.H. Peichl, M. Sayeh, and R. Touzani. A free boundary problem for the stokes equations. *ESAIM : Control, Optimisation and Calculus of Variations*, 23(1) :195–215, 2017.

[6] F. Boyer and P. Fabrie. *Mathematical Tools for the Study of the Incompressible Navier-Stokes Equations andRelated Models*, volume 183. Springer Science & Business Media, 2012.

[7] M.C. Delfour and J.P. Zolésio. Structure of shape derivatives for nonsmooth domains. *Journal of functional Analysis*, 104(1) :1–33, 1992.

[8] M.C. Delfour and J.P. Zolésio. *Shape and Geometries*. SIAM, 2002.

[9] K. Eppler and H. Harbrecht. On a kohn-voelius like formulation of free boundary problems. *Computational Optimization and Applications*, 52(1) :69–85, 2012.

[10] J. Fabricius. Stokes flow with kinematic and dynamic boundary conditions. *Quart. Appl. Math.*, 77(3) :525–544, 2019.

[11] J. Haslinger, T. Kozubek, K. Kunish K, and G. Peichl. Shape optimization and fictitious domain approach for solving free-boundary value problems of bernoulli type. *Comput. Optimiz. Appl.*, 26 :231–251, 2003.

[12] F. Hecht. New development in freefem++. *J. Numer. Math.*, 20(3-4) :251–265, 2012.

[13] A. Henrot and M. Pierre. *Shape Variation and Optimization*. European Mathematical Society Press, 2018.

[14] K. Ito, K. Kunish K, and G. Peichl. Variational approach to shape derivative for a class of bernoulli problem. *J. Math. Anal. App.*, 314 :126–149, 2006.

[15] A. Laurain and Y. Privat. On a bernoulli problem with geometric constraints. *ESAIM : Control, Optimisation and Calculus of Variations*, 18(1) :157–180, 2012.

[16] J.L. Lions. Problèmes aux limites dans les équations aux dérivées partielles, presses de l'université de montréal. *Montréal 1965. Zbl0143*, 14003, 1962.

[17] J.P. Lohéac. *Problèmes elliptiques à données peu régulières, applications*. PhD thesis, Université Claude Bernard-Lyon I, 2002.

[18] J. Simon. Differentiation with respect to the domain in boundary value problems. *Numerical Functional Analysis and Optimization*, 2(7-8) :649–687, 1980.

[19] J. Simon. Domain variations for drag in stokes flow. In X. Li et J. Yong, editor, *Control theory of distributed parameter systems and applications*, pages 28–42. Springer, 1991.

[20] J.P. Zolésio. An optimal design procedure for optimal control support. In Alfred Auslender, editor, *Convex Analysis and Its Applications*, pages 207–219, Berlin, Heidelberg, 1977. Springer Berlin Heidelberg.